# Kinetically driven shape changes in early stages of two-dimensional island coarsening: Ag/Ag(111)

Giridhar Nandipati,[*] Abdelkader Kara,[†] Syed Islamuddin Shah,[‡] and Talat S. Rahman[§]
*Department of Physics, University of Central Florida, Orlando, Florida 32816, USA*
(Received 31 December 2012; revised manuscript received 23 July 2013; published 3 September 2013)

We present here a detailed analysis of the shapes of two-dimensional Ag islands of various sizes observed during the early stages of coarsening on the Ag(111) surface, using kinetic Monte Carlo (KMC) simulations, and show that selectivity is due to the formation of kinetically stable island shapes that survive longer than nonselected sizes, which decay into nearby selected sizes. The stable shapes have a closed-shell structure—one in which every atom on the periphery has at least three nearest neighbors. These findings further explain our earlier study in which we found that in the early stages coarsening proceeds as a sequence of selected island sizes resulting in peaks and valleys in the island size distribution [G. Nandipati, A. Kara, S. I. Shah, and T. S. Rahman, J. Phys.: Condens. Matter **23**, 262001 (2011)]. This selectivity is dictated by the relative energetics of edge-atom diffusion and detachment and attachment processes and by the large activation barrier for kink detachment. Our simulations were carried out using a very large database of processes identified by each atom's unique local environment using the self-learning KMC scheme. The activation barriers were calculated using semiempirical interaction potentials based on the embedded-atom method.

DOI: 10.1103/PhysRevB.88.115402 PACS number(s): 68.35.Fx, 68.43.Jk, 81.15.Aa, 68.37.−d

## I. INTRODUCTION

The phenomenon of coarsening plays an important role in a wide variety of processes in many branches of the physical sciences. Of particular interest is coarsening of two-dimensional (2D) or three-dimensional (3D) islands on various surfaces. Given its technological importance, coarsening has been the subject of a great deal of experimental and theoretical investigation.[2–13] In recent years the development of fast scanning tunneling microscopes (STMs) has triggered the investigation of changes in surface morphologies that were deliberately created far from equilibrium,[14–24] as well as of thermal fluctuation around equilibrium-shaped structures[3,25–28] in high-temporal resolution. Room-temperature studies using STMs confirm that late-stage Ag/Ag(111) coarsening is dominated by Ostwald ripening,[17,22] which is driven by lowering of excess surface free energy associated with island edges, resulting in the growth of islands larger than a critical size at the expense of smaller islands.[29–32] Since these islands are assumed to be immobile, late-stage coarsening is considered to be mediated by diffusion of atoms between islands. Recently, through kinetic Monte Carlo (KMC) simulations using a large database of processes, we have shown that early stages of Ag(111) island coarsening, i.e, when islands are smaller in size, unlike late-stage coarsening, proceed as a sequence of selected island sizes.[1] This results in peaks at selected sizes and valleys at nonselected sizes in the island size distribution (ISD). We found that the islands of selected sizes do not have atoms diffusing along their edges. The fact that all atoms thus have at least three nearest neighbors and a closed-shell structure makes them kinetically stable and explains the peaks in the ISD at these sizes. The island selectivity was found to be independent of choice of initial ISD, initial shape of islands, and surface temperature, though the *strength* of the selectivity does depend on temperature. It should be noted that magic sizes have been observed during first stages of growth of Pt on Pt(111) above 500 K,[33] as well as in homoepitaxial growth on Si(111)[34] and Ag(111).[35] Interestingly, growth of magic sizes of 3D Pb nanocrystals on Si(111) leads to a breakdown of the classical Ostwald ripening laws.[23,24]

In this article, we extend our investigation to a detailed analysis of *shapes* of islands that we found to be stable during initial stages of homoepitaxial growth on the Ag(111) surface, and we discuss reasons why islands of certain sizes do not form kinetically stable shapes even if they are so favored through energetic considerations. We also present some additional proof that coarsening is mediated by diffusion of atoms between islands via adatom attachment and detachment processes. In contrast to a previous study[36] of the energetics of Ag clusters on Ag(111), we show that the kinetically stable island shapes do not necessarily have to be of the lowest energy.

The organization of this paper is as follows. In Sec. II we briefly describe self-learning kinetic Monte Carlo and the database of processes that we used in our simulations. In Sec. III we present results of our simulations of the initial stages of Ag/Ag(111) island coarsening and our understanding of reasons for island size selectivity. Specifically, we discuss how island size selectivity is governed by the relative energy barriers for various detachment processes which determine the shapes of islands of various sizes formed during coarsening. Finally, in Sec. IV we present our conclusions.

## II. SIMULATIONS

Kinetic Monte Carlo is an efficient method[37–42] for carrying out a wide variety of dynamical simulations of nonequilibrium processes when the relevant activated atomic-scale processes are known *a priori*. Accordingly, KMC simulations have been successfully used to model a variety of dynamical processes ranging from catalysis to thin-film growth over experimentally relevant length and time scales.

In our simulations we made use of a very large database of processes obtained from previous self-learning KMC (SLKMC)[43–45] simulations of small and large Ag-island diffusion on an Ag(111) surface carried out at temperatures of 300 and 500 K. This database contains a wide variety of single-, multi-, and concerted atom processes and has been

 

used earlier[11] for reliable long time scale KMC simulations (on the order of a few hundred seconds) of Ag island coarsening on Ag(111) at room temperature. All diffusion processes in this database move atoms from one fcc site to another. We used the embedded-atom method (EAM) as developed by Foiles *et al.*[46] to calculate the energy barriers for diffusion processes. Since rates are not expected to be strongly affected in the low-temperature regime explored, we introduced a simplification by assuming a "normal" value of $10^{12}$ $s^{-1}$ for all diffusion prefactors, although we are aware that multiatom processes may be characterized by high prefactors.[47–49] Rates are not expected to be strongly affected in the explored low- to moderate-temperature regime. Similar to our previous study[11] we used a relatively large system size of $1024 \times 1024$ fcc lattice units with periodic boundary conditions in order to avoid finite-size effects, and to get good statistics our results were averaged over ten runs. More details about database acquisition, types of processes with their respective activation energy barriers, recipes for speeding KMC simulations, and additional information about the simulation can be found in Ref. 11.

## III. RESULTS

### A. Initial configuration

We created the initial distribution of islands for our coarsening simulation by first dividing the empty lattice into boxes of equal size, then randomly selecting an island size and a box, and placing an island of that size at the center of that box, so as to prevent any overlap of islands. In our case we divided the lattice of size $32 \times 32$ into 1024 boxes. The total number of islands and the number of islands of a particular size in the distribution depend on the type of initial ISD chosen. We ran our simulations using both Gaussian and delta initial ISDs. In the delta initial distributions, we set all 742 islands at a given size (repeating the simulation for islands of all sizes between 10 and 30). For a Gaussian distribution the total number of islands depends on the number of islands ($a$) of average size, that is, the number of islands at the peak of the distribution ($\mu$) and the width of the distribution ($\sigma$). All island sizes between $\mu \pm \sigma\sqrt{2\ln(a)}$ are present in the distribution so that the distribution is uniform around the average island size. Figure 1 shows an example of a Gaussian initial island size distribution, this one with a peak of 100 islands at size 12 and width of 3.

For each initial Gaussian ISD we arbitrarily set the peak at 100 islands at the average size and set the width at 3. The result in each case for an initial Gaussian ISD is a total of 742 islands, the set of initial distributions differing from each other in the number of atoms set as the average size. That is, the total number of islands in the initial ISD is kept constant (742) for all simulations by keeping the peak island count and the width of the Gaussian distribution constant regardless of the average island size. For simplicity the shapes of islands in the initial ISD were chosen arbitrarily, and islands of the same size were assigned the same shape. The simulation was repeated for different shapes for a given island size. For the results presented here, most of the initial island shapes were either compact or close to compact. To ensure that our results were not a reflection of this choice of initial shapes, we ran another set of simulations in which the assigned shapes were fractal. The results between the two sets of simulations were indistinguishable.

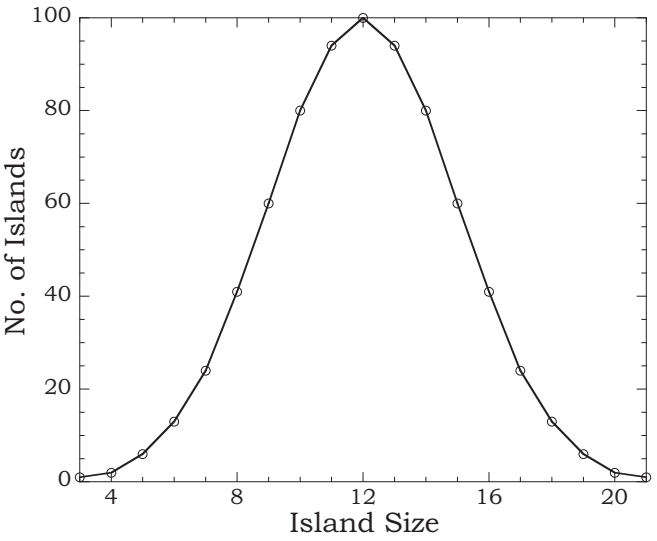


FIG. 1. Gaussian initial island size distribution with peak of 100 islands at size 12 and width of 3.

### B. Island size selectivity

We found that during early stages when island sizes are small coarsening proceeds as a sequence of selected island sizes,[1] as is clearly evident in Figs. 2 and 3, which show ISDs at various times when the starting ISDs are delta and Gaussian, respectively. We carried out these simulations up to 3.0 s. It can be seen that as the coarsening proceeds there is a dramatic change in the ISD from a sharp delta or a smooth Gaussian to a nonsmooth distribution, with peaks and valleys. Figures 2 and 3 also show that at some island sizes (19, 27, and 30 atoms) there is neither a peak nor a valley within the ISD. At either size 23 or 24 there can be a peak, though for the most part the peak occurs at size 23, while at size 24 there is neither a peak nor a valley. Table I summarizes island sizes up to 35 atoms after 1.0 s of coarsening according to whether they constitute a peak, valley, or neither within the ISD. Note that at much later times all island coarsening exhibits Ostwald ripening, resulting in a single large island: the total energy of the system will decrease as more bonds are formed until it saturates when one large island is formed. These characteristics of early- and late-stage coarsening are independent not only of whether the initial ISD is Gaussian or delta but also of whether it is random. We confirmed the latter by carrying out coarsening simulations with an initial ISD created by depositing Ag atoms on the Ag (111) surface at very low temperature (135 K) with a slightly higher monomer diffusion barrier to increase the number of islands and to keep the average island size smaller. Under these conditions islands are fractal and the ISD is random. The ISD exhibits the same characteristic change even when the shapes of islands are altered in the initial configuration, for example, to one that is kinetically stable or of low energy, or of an irregular shape. We also found that although the strength of selectivity depends on temperature there is no change with

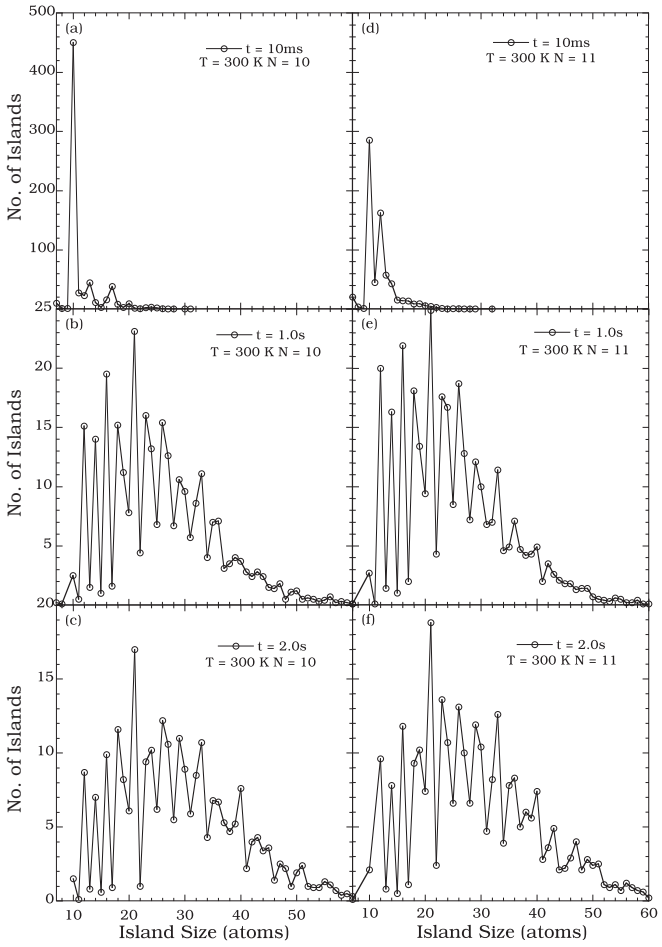


FIG. 2. ISDs at $T = 300$ K when the initial ISD is a delta function in which all 742 islands are of size 10 or size 11, respectively. (a), (d) 10 ms. (b), (e) 1.0 s. (c), (f) 2.0 s.

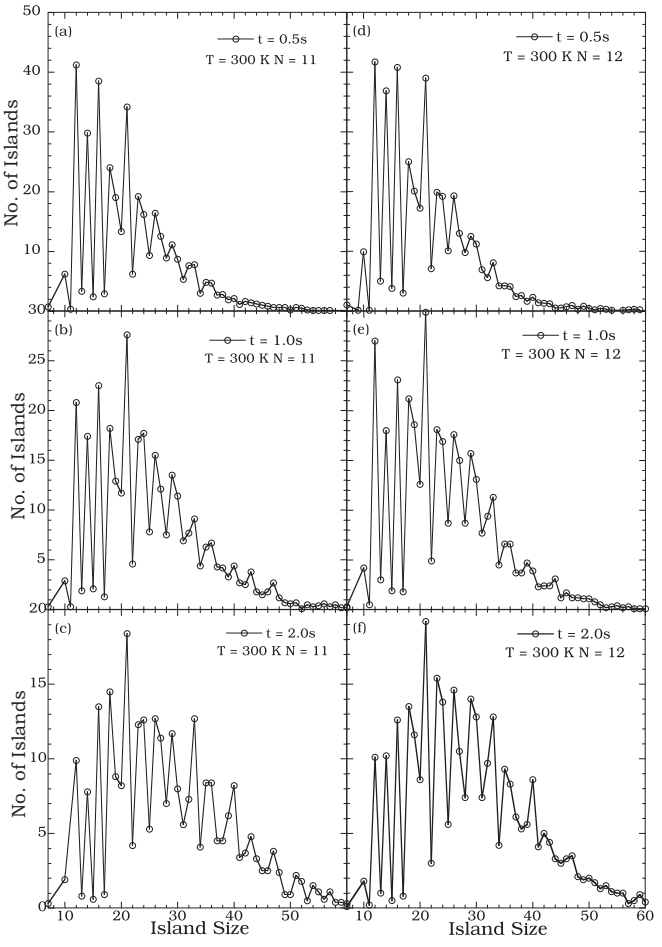


FIG. 3. ISDs at $T = 300$ K when the initial ISD is a Gaussian function in which average island size is 10 atoms or 11 atoms, respectively. (a), (d) 10 ms. (b), (e) 1.0 s. (c), (f) 2.0 s.

temperature in the sizes of islands that constitute peaks and valleys in the ISD. In sum (as our earlier study showed), island size selectivity is independent of all parameters of initial ISD, including temperature, island shape(s), and whether the distribution is random, delta, or Gaussian.

It is known[11,13,17] that for two-dimensional Ag islands late-stage coarsening on the Ag(111) surface is due to evaporation and condensation mediated by monomer diffusion between islands. To elucidate the factors that determine the pattern of island size selectivity described above during early-stage coarsening, we examined the energetics of detachment processes on the basis of island sizes from 8 through 21. [For islands whose sizes are smaller than eight atoms, the energy barriers for the most frequent concerted diffusion processes are quite small (0.1–0.3 eV), causing these islands to diffuse and coalesce with others.] Figure 4 shows histograms of energy barriers for detachment events that are selected during 3.0 s of coarsening for sizes 11 through 14 when the initial ISD was a Gaussian. Note that one can discover a one-to-one correspondence between the histograms in Fig. 4 and the actual calculated barriers for the most frequent edge-atom detachment processes (Fig. 3 in Ref. 1). That is, in Fig. 4, 0.275 eV corresponds to the activation barrier for detachment of a corner atom, 0.475 eV corresponds to that for detachment of an edge atom from a $B$-type step edge, and barriers 0.525 and 0.575 eV correspond to those for detachment of an edge atom from an $A$-type step edge. Also, the difference (Fig. 3 in Ref. 1) between an edge diffusion barrier and an edge-atom detachment barrier is quite small on a $B$-type step edge, making it the most frequent type of detachment process. Recall (from Figs. 2 and 3) that the populations of islands of sizes 11 and 13 atoms constitute valleys while those of islands of sizes 12 and 14 atoms constitute peaks in the ISD. Now, comparing the height of the histogram in Fig. 4(a) with that in Fig. 4(c) and that in Fig. 4(b) with that in Fig. 4(d), we see that the number of events of edge-atom detachment for island sizes whose populations constitute valleys in the ISD is much higher than that for island sizes whose populations constitute peaks in the ISD. The reason is that because the energy barrier for

TABLE I. List of island sizes for which the ISD is a peak, a valley, or neither after 3.0 s coarsening (taken from Ref. 1).

| Feature | Sizes of islands | | | | | | | | | |
|---|---|---|---|---|---|---|---|---|---|---|
| Valley | 11 | 13 | 15 | 17 | 20 | 22 | 25 | 28 | 31 | 34 |
| Peak | 12 | 14 | 16 | 18 | 21 | 23(24) | 26 | 29 | 33 | 35 |
| Neither | | | | 19 | | | 27 | 30 | 32 | |

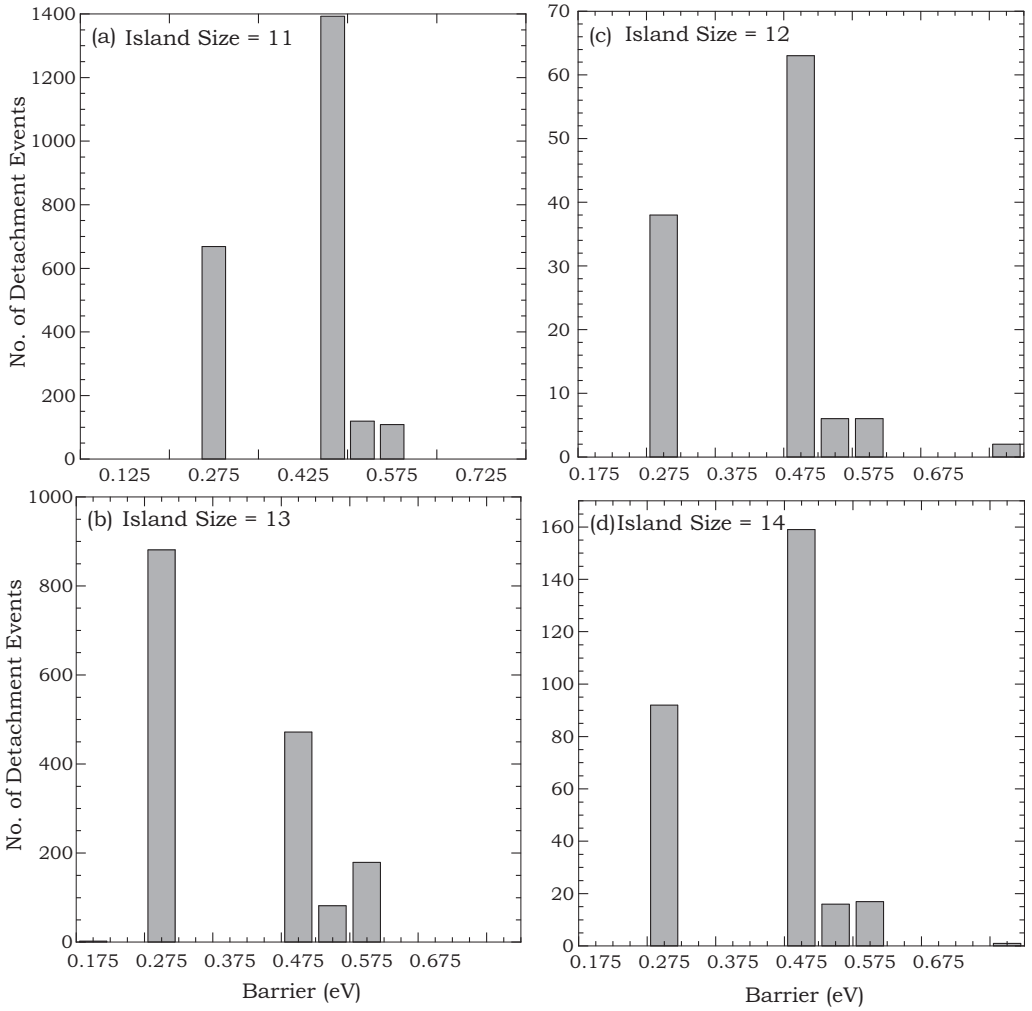


FIG. 4. Histogram of detachment events selected for islands of size (a) 11 atoms, (b) 12 atoms, (c) 13 atoms, and (d) 14 atoms during 3 s of coarsening. The histogram interval is 0.05 eV.

an atom with at least three nearest-neighbor atoms to detach is greater than 0.7 eV such atoms rarely detach to create monomers at room temperature. These arguments based on system energetics confirm findings in our KMC simulations that islands of sizes whose populations are peaks in the ISD have no edge atoms: instead, all their atoms have at least three nearest-neighbor atoms, making them kinetically stable islands. We also found that artificially increasing the energy barrier for the most frequent detachment processes delays the onset of island selectivity to later times. Accordingly, we conclude that island size selection is primarily due to adatom detachment and attachment processes at island boundaries owing to the relative ease with which edge atoms can detach in comparison with the relative difficulty for the detachment of atoms with at least three nearest-neighbor atoms.

### C. Shape analysis

In order to gain further insight into island size selectivity we looked at shapes of islands as a function of their size. Shapes an island can assume during coarsening are constrained by the fact that detachment events are predominately edge-atom detachments and rearrangement of atoms in an island rarely happens due to the high detachment barrier for atoms with at least three nearest neighbors. We use the term "compact shape" to specify a shape with a closed-shell structure, i.e., one with no edge atoms or kinks. As already mentioned, islands of sizes smaller than eight atoms are hardly present since they quickly diffuse and coalesce with other islands. Therefore we follow the shapes starting from islands of size 10 atoms, which is the first stable size after islands of size 8 atoms, all the way up to islands of size 21 atoms. In order to uniquely identify the shape of the island spontaneously, we used the following three criteria: (1) the number of nearest neighbors, (2) the maximum distance of any atom from the center of mass of the island, and (3) the maximum distance between any two atoms in the island. Most often criteria 1 and 2 are sufficient to uniquely identify the shape of an island.

Figure 5(a) shows the most frequent shape observed for islands of size 10 atoms during coarsening. There are two other possible orientations for this shape which can be obtained by rotating the shape shown in Fig. 5(a) by 120 or 240° either clockwise or anticlockwise about the center of mass of the island. For brevity we will show only one of the possible

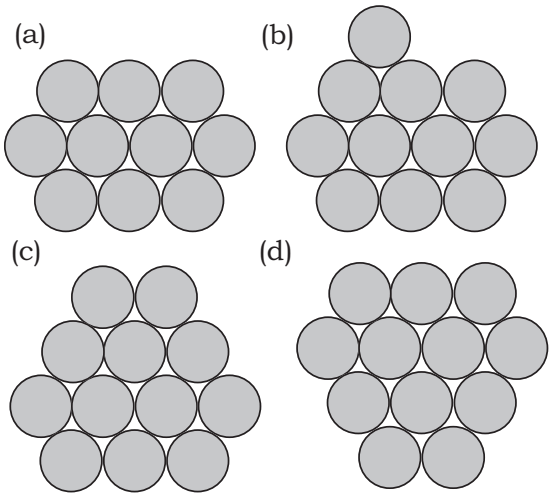


FIG. 5. The most frequent shapes for islands of size (a) 10 atoms, (b) 11 atoms, (c) 12 atoms, and (d) 12 atoms. Note that in (c) the *B*-type step edge is longer than the *A* type, while in (d) the opposite is the case.

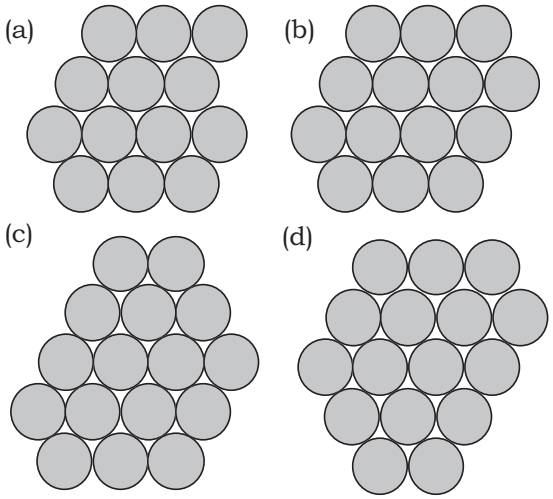


FIG. 6. Shapes of islands of sizes (a) 13 atoms, (b) 14 atoms, (c) 16 atoms (longer *B*-type step edge), and (d) 16 atoms (longer *A*-type step edge).

orientations. We note that the barrier for a monomer to attach to an *A*-type step edge (0.04 eV) is smaller than the barrier for it to attach to a *B*-type step edge (0.06 eV). Also it can be seen (Fig. 3 in Ref. 1) that the barrier for an edge atom to detach from a *B*-type step edge is slightly smaller than that at an *A*-type step edge. Since it is relatively easier for a monomer to attach and harder for it to detach from an *A*-type step edge, the most frequent shape observed for islands of size 11 atoms is as shown in Fig. 5(b), with an edge atom on an *A*-type step edge. An 11 atom island with an edge atom on a *B*-type step edge can also form during coarsening, but it changes relatively quickly to an island of size 10 atoms through detachment or rarely to a 12 atom island due to attachment of a monomer. Similarly, Fig 5(c) shows the most frequent shape observed for islands of size 12 atoms, which forms when a monomer attaches to the kink on the most frequent shape of island of size 11 atoms [Fig. 5(b)], resulting in a longer *B*-type step edge. Figure 5(d) shows the next most frequent shape for islands of size 12 atoms, with longer *A*-type step edges, which is formed when a monomer attaches to the kink on a *B*-type step edge on the less frequent shape of an 11 atom island. Since the two most frequent shapes for islands of size 12 atoms are compact and survive much longer, their population constitutes a peak in the ISD. We note that shapes shown in Figs. 5(c) and 5(d) are the only possible kinetically stable shapes for a 12 atom island while that for the 10 atom island is shown in Fig. 5(a).

Figure 6(a) shows the most frequent shape observed for islands of size 13 atoms during coarsening. It can be seen that its shape is a combination of a 12 atom island with a longer *B*-type step edge and one extra edge atom. This edge atom can either easily detach to form an island of size 12 atoms or a monomer can attach to it to form an island of size 14 atoms, so that the populations of islands of size 13 atoms constitute a valley in the ISD. Figure 6(b) shows the most frequent shape for an island of size 14 atoms. This shape and its other two orientations (rotated by 120 and 240°) can also be formed by attaching two atoms to the step edges to either of two shapes shown in Figs. 5(c) and 5(d) for islands of size 12 atoms, resulting in the same shape for islands of size 14 atoms, with two longer *A*-type and *B*-type step edges. Figures 6(c) and 6(d) show the two most frequent shapes for islands of size 16 atoms, one with a longer *B*-type step edge and the other with a longer *A*-type step edge, respectively. These shapes are formed when two atoms attach to *A*-type and *B*-type step edges, respectively, of a 14 atom island shown in Fig. 6(b). As mentioned earlier, since it is easier for a monomer to attach to an *A*-type step edge compared to a *B*-type step edge, the shape of a 16 atom island shown in Fig. 6(c) is the most frequent observed shape. Since the most frequent shapes for islands of size 16 atoms are compact, their populations constitute a peak in the ISD, and any monomer that attaches to the step edge easily detaches, with the consequence that the populations of islands of size 17 atoms constitute a valley in the ISD. We again note that Fig. 6(b) shows the only possible kinetically stable shape for a 14 atom island while Figs. 6(c) and 6(d) show that for a 16 atom island.

Figure 7 shows the most frequent shapes observed for islands of size 18 atoms during coarsening. These shapes are formed when two atoms attach to one of the step edges of islands of size 16 atoms shown in Figs. 6(c) and 6(d). The most frequent shapes for islands of size 18 atoms are the compact ones, and therefore their populations constitute a peak in the ISD. These frequent shapes are also the only kinetically stable shapes possible for an 18 atom island. Since islands of size 18 atoms are compact, one expects populations of islands of size 19 atoms to constitute a valley in the ISD. But islands of size 18 atoms, though less frequently, also form noncompact shapes shown in Figs. 7(c) and 7(f). These noncompact shaped islands are relatively stable against detachment of an atom, but any monomer that attaches to the island is absorbed at the kink to form a compact and kinetically stable hexagonal shaped 19 atom island. Hexagonal shaped 19 atom islands are extremely stable once formed and are hence the most frequently observed type of 19 atom islands. Accordingly, as can be seen from Figs. 2 and 3, the populations of islands of size 19 atoms constitute neither a peak nor a valley in the ISD. We note that Fig. 7(a) is the most frequent shape for islands

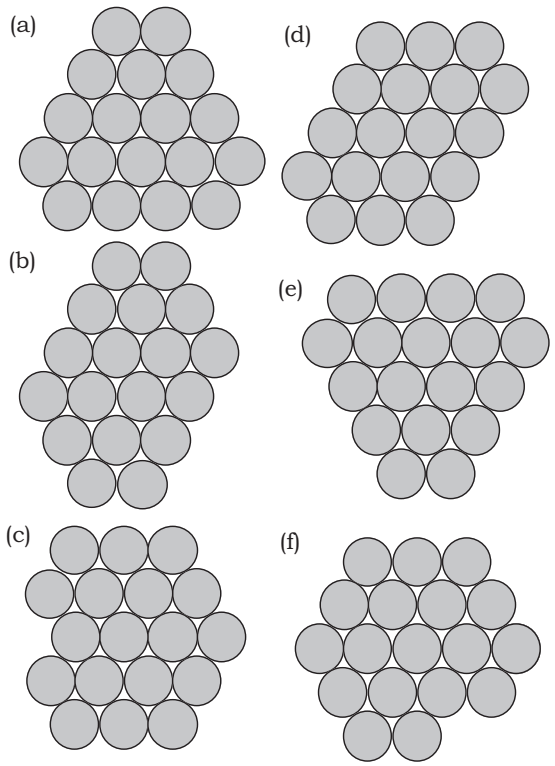


FIG. 7. The most frequent shapes observed for islands of size 18 atoms.

of size 18 atoms, while shapes in Figs. 7(b) and 7(d) are less frequently observed compact shapes.

Figures 8(a) and 8(b) show compact shapes observed for islands of size 20 atoms during coarsening. These shapes are formed when two atoms attach to the shorter step edge (three atoms wide) of islands of size 18 shown in Figs. 7(b) and 7(d). Other shapes that form most often for islands of size 20 atoms during coarsening are not compact: they have either an edge atom or a kink. These noncompact shapes quickly change to islands of either size 18 or 19 atoms, due to detachment, or size 21 atoms, due to attachment of a monomer. Figure 9 shows the most frequent shapes for islands of size 21 atoms observed during coarsening. It can be easily checked that these shapes can be obtained by attaching three atoms to longer edges [Figs. 7(a), 7(b), 7(d), and 7(e)] and two atoms to any step edge of a hexagonal shaped 19 atom island. In particular, all shapes shown in Fig. 7 lead to shapes shown in Fig. 9 for

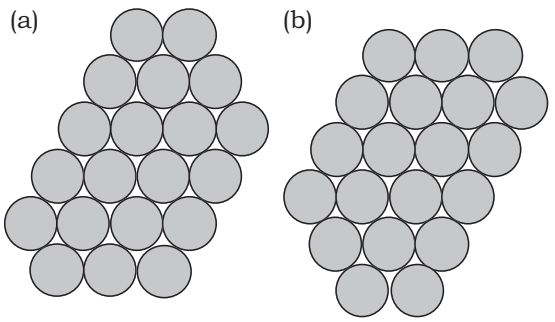


FIG. 8. The most frequent shapes of islands of size 20 with longer (a) *B*-type and (b) *A*-type step edges.

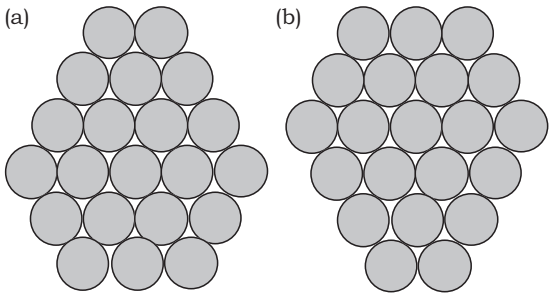


FIG. 9. The most frequent shapes of islands of size 21 with longer (a) *B*-type and (b) *A*-type step edges.

islands of size 21 atoms. As can be seen in Figs. 2 and 3, this leads to a very sharp population peak at islands of size 21 atoms in the ISD.

Note that as a result of a high detachment barrier for atoms with at least three nearest neighbors, these atoms rarely detach to create monomers, and that atoms in an island do not rearrange except through attachment and detachment of edge atoms. Therefore, whether an island takes a particular shape or not depends on the shapes of islands smaller than it formed during coarsening. Moreover, certain nonselected island sizes for which a kinetically stable shape might exist appear only rarely, since except through atom detachment these islands are not able to rearrange themselves into a kinetically stable shape. For example, for an island of size 13 atoms, Fig. 6(a) shows the most frequent shape observed during coarsening while Fig. 10(a) shows the only kinetically stable shape possible. Figures 10(b)–10(d) show other kinetically

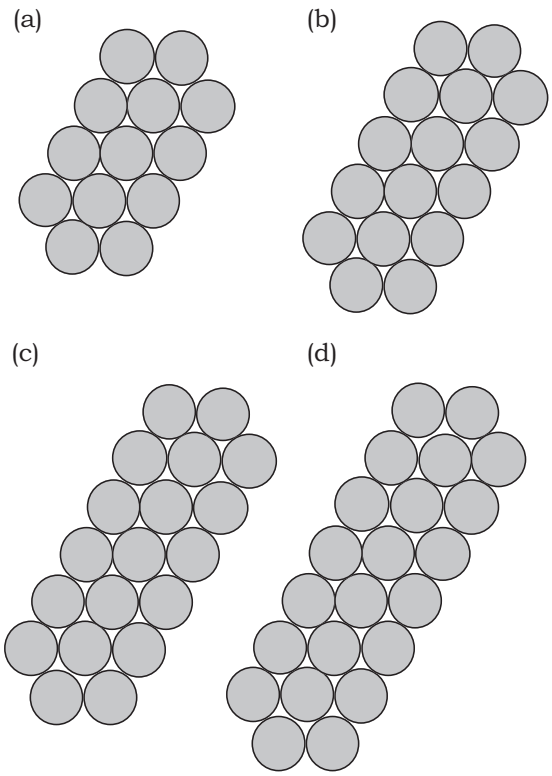


FIG. 10. Less frequent kinetically stable shapes for island size (a) 13, (b) 16, (c) 19, and (d) 22.

stable shapes possible which do not appear during coarsening for islands of sizes 16, 19, and 22, respectively. For an island of size 20 atoms, because of the presence of compact island shapes [Figs. 8(a) and 8(b)] it can be seen that its population density is nonzero even though it constitutes a valley in the ISD. It can also be seen, in Figs. 2 and 3, that islands of sizes 11, 13, 15, and 17 atoms, which never form a compact shape during coarsening, usually have zero population density. For islands of size 11, 15, and 17 atoms, compact shapes are a geometric impossibility. Accordingly, we conclude that island selection is primarily due to edge-atom detachment and attachment processes at island boundaries owing to the relative ease with which atoms can detach in comparison with the relative difficulty for the detachment of atoms with at least three nearest neighbors.

## IV. CONCLUSIONS

We find that during early stages, when island sizes are small, two-dimensional Ag island coarsening on the Ag(111) surface proceeds as a sequence of selected island sizes resulting in peaks and valleys in the ISD. Densities of islands of selected sizes decay at slower rates because of the formation of kinetically stable island shapes, while densities of nonselected sizes (valleys in the ISD) decay more rapidly owing to nonformation of selected island shapes. A kinetically stable shape has a closed-shell structure, with all periphery atoms having at least three nearest-neighbor bonds (no kinks), thus making the detachment of a periphery atom a rare process. Consequently their densities decay at a slower pace. In contrast, densities of nonselected sizes decay more rapidly owing to a higher frequency of edge-atom attachment and detachment processes, which are either single or doubly bonded atoms and easier to detach, resulting in the creation of monomers.

Although kinetically unstable shapes of a selected island size are formed during coarsening, their densities are negligible compared to the density of kinetically stable shapes. Kinetically stable islands once formed do not rearrange into other shapes, since they do not have any kink in their shapes, which makes it difficult for a periphery atom to detach even to form an edge diffusing atom. However, if there is a kink at the periphery of an island, the kink atom may transform into an edge atom, which can detach to form a monomer or the kink may disappear by the attachment of an edge atom created due to the attachment of a monomer. As the coarsening proceeds, island sizes get bigger, the number of shapes an island can assume become larger, and each island size can have multiple kinetically stable shapes. In our coarsening simulations we have found that island selectivity is clearly visible until island sizes of 30–40 atoms, beyond which the island population densities are so small that selectivity is not noticeable.

Coarsening results presented in this article were started with ISDs created manually with Gaussian distribution. We observed the same island size selectivity when the initial ISD was created by deposition at a very low temperature, and islands formed have fractal shapes. Furthermore the island size selectivity was independent of parameters of initial ISD such as average island size, island shapes, and the type of distribution, showing that it is a characteristic of the early stage of Ag island coarsening on Ag(111). In addition we found that, though island size selectivity was qualitatively independent of temperature, quantitatively it is strongest between 250 and 270 K. Beyond 300 K, island density decays so fast that selectivity was barely observable. In conclusion, kinetically stable island sizes found in our KMC simulations can be rationalized on the basis of the propensity of the two-dimensional island to sustain atom attachment and detachment processes. Our work also points to the importance of consideration of the kinetics of diffusion processes together with their energetics.

## ACKNOWLEDGMENTS

This work was initiated with partial funding from NSF Grant No. ITR-0840389 and completed under funding from US Department of Energy Grant No. DE-FG02-07ER46354. We would also like to acknowledge computational resources provided by the STOKES facility at the University of Central Florida. We thank Lyman Baker for critical reading of the manuscript.

*giridhar.nandipati@pnnl.gov
†abdelkader.kara@ucf.edu
‡islamuddin@knights.ucf.edu
§talat.rahman@ucf.edu

[1] G. Nandipati, A. Kara, S. I. Shah, and T. S. Rahman, J. Phys.: Condens. Matter **23**, 262001 (2011).
[2] M. Zinke-Allmang, L. C. Feldman, and M. H. Grabow, Surf. Sci. Rep. **16**, 377 (1992).
[3] W. W. Pai, A. K. Swan, Z. Zhang, and J. F. Wendelken, Phys. Rev. Lett. **79**, 3210 (1997).
[4] S. V. Khare, N. C. Bartelt, and T. L. Einstein, Phys. Rev. Lett. **75**, 2148 (1995).
[5] P. Meakin, Physica A **165**, 1 (1990).
[6] J. M. Soler, Phys. Rev. B **53**, R10540 (1996).
[7] D. S. Sholl and R. T. Skodje, Physica A **231**, 631 (1996).
[8] D. S. Sholl and R. T. Skodje, Phys. Rev. Lett. **75**, 3158 (1995).
[9] D. Kandel, Phys. Rev. Lett. **79**, 4238 (1997).
[10] G. R. Carlow and M. Zinke-Allmang, Phys. Rev. Lett. **78**, 4601 (1997).
[11] G. Nandipati, Y. Shim, J. G. Amar, A. Karim, A. Kara, T. S. Rahman, and O. Trushin, J. Phys.: Condens. Matter **21**, 084214 (2009).
[12] F. Shi, Y. Shim, and J. G. Amar, Phys. Rev. E **76**, 031607 (2007).
[13] K. Morgenstern, G. Rosenfeld, and G. Comsa, Surf. Sci. **441**, 289 (1999).
[14] D. R. Peale and B. H. Cooper, J. Vac. Sci. Technol. A **10**, 2210 (1992).
[15] W. Theis, N. C. Bartelt, and R. M. Tromp, Phys. Rev. Lett. **75**, 3328 (1995).

[16]N. C. Bartelt, W. Theis, and R. M. Tromp, Phys. Rev. B **54**, 11741 (1996).
[17]K. Morgenstern, G. Rosenfeld, and G. Comsa, Phys. Rev. Lett. **76**, 2113 (1996).
[18]J. M. Wen, S.-L. Chang, J. W. Burnett, J. W. Evans, and P. A. Thiel, Phys. Rev. Lett. **73**, 2591 (1994).
[19]J. B. Hannon, C. Klunker, M. Giesen, H. Ibach, N. C. Bartelt, and J. C. Hamilton, Phys. Rev. Lett. **79**, 2506 (1997).
[20]A. Ichimiya, Y. Tanaka, and K. Ishiyama, Surf. Sci. **386**, 182 (1997).
[21]M. Giesen, G. Schulze Icking-Konert, and H. Ibach, Phys. Rev. Lett. **80**, 552 (1998).
[22]K. Morgenstern, G. Rosenfeld, E. Laegsgaard, F. Besenbacher, and G. Comsa, Phys. Rev. Lett. **80**, 556 (1998).
[23]C. A. Jeffrey, E. H. Conrad, R. Feng, M. Hupalo, C. Kim, P. J. Ryan, P. F. Miceli, and M. C. Tringides, Phys. Rev. Lett. **96**, 106105 (2006).
[24]G. P. Zhang, M. Hupalo, M. Li, C. Z. Wang, J. W. Evans, M. C. Tringides, and K. M. Ho, Phys. Rev. B **82**, 165414 (2010).
[25]M. Poensgen, J. F. Wolf, J. Frohn, M. Giesen, and H. Ibach, Surf. Sci. **274**, 430 (1992).
[26]L. Kuipers, M. S. Hoogeman, and J. W. M. Frenken, Phys. Rev. Lett. **71**, 3517 (1993).
[27]K. Morgenstern, G. Rosenfeld, B. Poelsema, and G. Comsa, Phys. Rev. Lett. **74**, 2058 (1995).
[28]W. W. Pai, N. C. Bartelt, and J. E. Reutt-Robey, Phys. Rev. B **53**, 15991 (1996).
[29]W. Ostwald, Z. Phys. Chem. **37**, 385 (1901).
[30]P. W. Voorhees, J. Stat. Phys. **38**, 231 (1985).
[31]I. M. Lifshitz and V. V. Slyozov, J. Phys. Chem. Solids **19**, 35 (1961).
[32]C. Wagner, Z. Elektrochem. **65**, 581 (1961).
[33]G. Rosenfeld, A. F. Becker, B. Poelsema, L. K. Verheij, and G. Comsa, Phys. Rev. Lett. **69**, 917 (1992).
[34]B. Voigtlander, M. Kastner, and P. Smilauer, Phys. Rev. Lett. **81**, 858 (1998).
[35]K. Morgenstern, E. Laegsgaard, and F. Besenbacher, Phys. Rev. Lett. **94**, 166104 (2005).
[36]E. Hristova, V. G. Grigoryan, and M. Springborg, Surf. Sci **603**, 3339 (2009).
[37]A. B. Bortz, M. H. Kalos, and J. L. Lebowitz, J. Comput. Phys. **17**, 10 (1975).
[38]G. H. Gilmer, J. Crystal. Growth. **35**, 15 (1976).
[39]A. F. Voter, Phys. Rev. B **34**, 6819 (1986).
[40]P. A. Maksym, Semiconf. Sci. Technol. **3**, 594 (1988).
[41]K. A. Fichthorn and W. H. Weinberg, J. Chem. Phys. **95**, 1090 (1991).
[42]J. L. Blue, I. Beichl, and F. Sullivan, Phys. Rev. E **51**, R867 (1995).
[43]O. Trushin, A. Karim, A. Kara, and T. S. Rahman, Phys. Rev. B **72**, 115401 (2005).
[44]A. Karim, A. N. Al-Rawi, A. Kara, T. S. Rahman, O. Trushin, and T. Ala-Nissila, Phys. Rev. B **73**, 165411 (2006).
[45]A. Kara, O. Trushin, H. Yildirim, and T. S. Rahman, J. Phys.: Condens. Matter **21**, 084213 (2009).
[46]S. M. Foiles, M. I. Baskes, and M. S. Daw, Phys. Rev. B **33**, 7983 (1986).
[47]H. Yildirim, A. Kara, and T. S. Rahman, Phys. Rev. B **76**, 165421 (2007).
[48]G. Henkelman and H. Jónsson, Phys. Rev. Lett. **90**, 116101 (2003).
[49]F. Montalenti, Surf. Sci. **543**, 141 (2003).